IEEE Access
Multidisciplinary ⋮ Rapid Review ⋮ Open Access Journal

Received November 10, 2021, accepted December 1, 2021, date of publication December 3, 2021,
date of current version December 16, 2021.

Digital Object Identifier 10.1109/ACCESS.2021.3132659

A Low Voltage Single Phase Online Uninterruptible Power Supply System Based on APFC and Fuzzy PID Algorithm

SHENGXIAN XU[1], CHEN LI[2], (Member, IEEE), YURU WANG[1], AND BAOYING LI[1], (Member, IEEE)

[1]School of Information Science and Engineering, Dalian Polytechnic University, Dalian 116034, China
[2]School of Electrical Engineering and Telecommunications, University of New South Wales (UNSW Sydney), Sydney, NSW 2052, Australia

Corresponding author: Yuru Wang (wangyr@dlpu.edu.cn)

ABSTRACT The Uninterruptible Power Supply (UPS) is a kind of power supply with electric energy storage, but most UPS systems bring harmonic pollution to the grid, and the power factor is inaccurate in the boost circuit, the output voltage is unstable. Therefore, an active power factor correction circuit (APFC) based on the current and voltage double closed-loop structure is designed in the boost circuit; besides, the fuzzy PID control algorithm is also proposed in the inverter circuit. The effectiveness of the proposed method can be verified by the computer simulation and real experiments, and there are four main results as follows. Firstly, the actual power factor of the UPS system can reach more than 0.996 with APFC correction circuit; then, the UPS system has the strong robustness and the shorter response time; in addition, the voltage regulation rate of the system remains at 0.083% and the load regulation rate is around 0.056%. Finally, the designed UPS system can provide the stable 36V $\pm$ 0.2V (50 $\pm$ 0.2Hz) AC power.

INDEX TERMS Low voltage, single phase, online UPS system, active power factor correction, fuzzy PID algorithm.

I. INTRODUCTION

The Uninterruptible Power Supply (UPS) system is a kind of energy storage device in emergency situation and sudden disconnection. It is mainly used to provide power stability in emergency management [1] and disaster relief [2]. In UPS system, it can convert DC power into AC power through the boost circuit and the inverter circuit [3]. The storage battery comprises several batteries in series. When the power supply works normally, the power is stored in the battery of UPS system. If the power supply cannot be supplied, the stored power immediately converted and supplied to the users [4]. The inverter generates the AC power by converting DC power. The isolation transformer can be used to isolate the interference of the grid, and its primary and secondary sides are completely insulated to prevent the input voltage drop, filter out the harmonic at the load-end, and improve the power supply quality [5]–[9].

However, there are some following problems in UPS system. The first is how to improve the power factor and reduce the harmonic pollution in the boost circuit. The second one is how to eliminate the output response instability and delay in UPS system [10]–[12].

Many scholars put forward a variety approaches to solve the first problem. Most UPS systems have no efficient solution to the use of electric energy in the boost circuit, the output of UPS system also has large voltage fluctuations, and the response to load change is slow. The UPS system cannot make the output voltage constant when the load changes suddenly. Reference [13] proposed the push-pull topology and double closed-loop control law in the DC-DC converter and it also designed the APFC correction circuit. The APFC correction with fixed turn-on time was designed using the average current mode control technology, and it kept the input current waveform synchronized with the voltage waveform and make the output DC voltage waveform smoother, and the power factor is about 0.96 [14]. Reference [15] mainly studied how to suppress the harmonic current and improve the power factor by adopting the voltage and current double closed-loop controller. Reference [16] described that the voltage and current double closed-loop control strategy were used in the APFC correction in the boost circuit, but

The associate editor coordinating the review of this manuscript and approving it for publication was Lei Wang.

the power factor reached around 0.98 and the Total Harmonic Distortion (THD) remained a higher level between 2.02% and 3.74%. In addition, the improved constant on-time (COT) control algorithm was proposed to improve the power factor [17]. References [18], [19] presented a simplified sinusoidal UPS system with a high-power factor, low total harmonic distortion and good dynamic response. Reference [20] designed an efficient power factor correction rectifier. Reference [21] proposed the variable duty cycle control method of four-channel interleaved power factor correction converter in the boost circuit, so that the system had the fast transient response, realized unity power factor, and had fast input and load transient response. References [13], [22] proposed a three-phase buck rectifier to improve the power factor of the system, the power utilization efficiency and system reliability, and reduce the DC link voltage of the grid. However, Ref. [22] used the active power control strategy by adjusting virtual resistance to solve DC over-voltage and uneven power distribution. Reference [23] proposed the online UPS system to adopt dual-mode operation, and it also used to improve the power factor of the inverter system. Reference [24] proposed an online UPS based on Z-source, and designed a broader range of input changes with the compensation of power fluctuation to improve the input power factor. In addition, Ref. [37] proposed a low-cost online UPS system to modify the sine wave and it was suitable for a load of switching power supply without power factor correction circuit.

Moreover, it is the objective to solve the problem of unstable output response and delay of UPS system, Ref. [6], [30]–[41] adopted a variety of control strategies in the inverter circuit. As for the online UPS system, Ref. [6] proposed a fast current control algorithm to suppress the surge current generated when the load was turned on or off. References [28], [29] used the traditional PID algorithm to output stable voltage. References [30]–[36] studied a variety of control algorithms to improve the robustness and adaptive ability of the system and effectively track voltage and current. However, the proposed control strategies in Ref. [30]–[36] such as synovial control, robust continuous control, model predictive control and neural network control were complex and difficult to transplant, with great limitations in scope of application and long development cycle, and it was difficult to develop the practical UPS productions. Reference [30] applied the synovial control theory with the problem of switching delay in practical application. Reference [31] proposed the robust continuous control and the model predictive control to track the output voltage of the inverter, but there was one problem in low utilization efficiency of the power supply. Reference [32] put forward control strategies such as PID control, repetitive control, deadbeat control and intelligent control. Reference [33] proposed the combination of PID and neural network in the power control system to improve its adaptive ability. Reference [34], [35] proposed SPWM technology to adjust the output of inverter, and they also proposed the fuzzy PID control algorithm to remain the amplitude of inverter output voltage. Reference [36] proposed PID algorithm to track the output voltage in the inverter circuit. References [12], [25]–[27] effectively tracked the output voltage in the inverter by using SPWM technology and the fuzzy PID algorithm. Reference [38] designed a single-phase online UPS system with low load regulation, and it proposed the closed-loop PID algorithm with DC voltage and AC voltage. In addition, compared with Synchronous Reference Frame (SRF), the fuzzy PID controller had a simple principle, robust adaptability and portability, certain robustness to load changes and robust fault tolerance [39], [40]. Reference [39] proposed a novel online maximum duty cycle tracking technology to reduce the cycle loss and switching loss of the converter and improve the efficiency of the server. In order to obtain the same holding time, it was also necessary to increase the DC link capacitance to increase the circuit volume and the mass. Reference [40] used a phase-locked loop structure (PLL) based on the current SRF algorithm to generate reference output voltage and unit vector coordinates. The single-phase PLL system was studied as a two-phase stationary coordinate system, and the control algorithms for generating orthogonal voltage were also proposed. Three of them used instantaneous peak detectors to generate quadrature voltages. Compared with the online topology with two cascaded PWM power converters operating at full power rating, the rating was processed by series and parallel converters in standby mode. However, the algorithm in Ref. [40] was complex so that it could not be widely used in practical use. Moreover, the current based the SRF algorithm is affected by the PLL structure, which consisted of the phase detector, the filter and the voltage-controlled oscillator and made the whole system more complex and it was difficult to build mathematical and simulation models. Reference [41] adopted the multi-loop control structure of the proportional controller with coordinate transformation and it also used two nested proportional controllers in the synchronous coordinate system. Reference [42] proposed a new uni-polar boost inverter topology, and it also used the direct zero vector of the inverter bridge, coupled inductor energy storage and transfer boost technology to realize the boost regulation of the inverter DC bus voltage and make the AC output voltage higher than the DC input voltage.

There are two proposed contributions in this paper:

1) In the boost circuit, we propose a voltage-current double closed-loop active power factor correction APFC) method, which can effectively improve the power factor and reduce the harmonic pollution in the power grid;
2) In the inverter circuit, we propose the fuzzy PID control algorithm with a higher response, which improves the response speed and ensures the stability of the output voltage.

The remainder of the paper is organized as follows. Section II presents the system model and formally states the considered problems. Section III presents the proposed algorithm with theoretical analysis, and Section IV demonstrates the performance of this algorithm via simulations

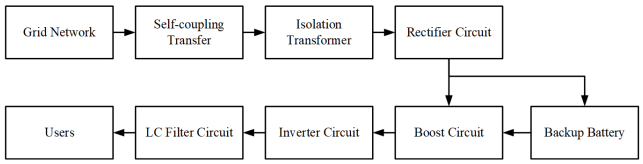

FIGURE 1. The physical overall model of the UPS system.

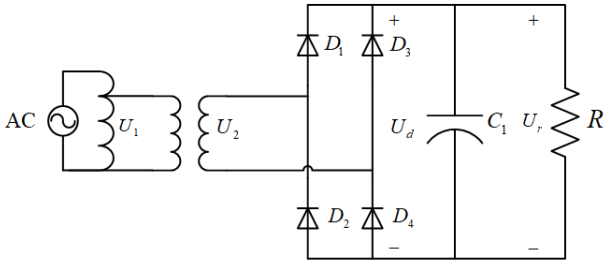

FIGURE 2. The model of uncontrollable rectifier circuit.

and the real experiment, including the power factor and output dynamic response characteristics of online single-phase UPS (the influence of voltage amplitude, frequency, response time, input voltage change and output load change). Finally, Section V briefly concludes this paper.

II. SYSTEM MODEL AND PROBLEM STATEMENT

A. THE OVERALL PHYSICAL MODEL OF THE UPS SYSTEM

The single-phase on-line UPS mainly includes the rectifier circuit, the boost circuit, the inverter circuit, the LC filter circuit and the backup battery circuit, and its physical overall model is shown in Fig. 1, in which, the self-coupling transfer reduces the 220V AC from the urban power supply network to 18V AC. The isolation transformer can isolate 18V AC from the rectifier circuit, the boost circuit, the inverter circuit and the users. The rectifier circuit rectifies and filters the alternating current in full wave and outputs about 25.443V DC. The boost circuit boosts 25.443V DC to 63V DC. The inverter circuit adopts a full bridge circuit and it outputs stable 36V AC through LC filter circuit. The MOSFET in the full bridge circuit is driven by IRF3205 and IR2104 chips. IRF3205 has small parasitic capacitance and can reduce switching loss, and its drain-to-source on-resistance is 0.008, and the switching frequency can reach 100kHz, which can quickly change the switching state. Moreover, the gate driving voltage of MOSFET is driven by IR2104 with bootstrap circuit. In addition, when the power supply disconnects, the backup battery immediately supplies power to the booster circuit, the inverter circuit as well as users.

B. THE RECTIFIER CIRCUIT

In this subsection, the uncontrollable rectifier circuit is shown in Fig. 2, in which, AC power generates the input voltage, U_1 denotes the output voltage of self-coupling transfer. D_1, D_2, D_3, and D_4 are the rectifier diodes, and these diodes compose the full-bridge rectifier circuit. U_2 is rectified to U_d, and U_r denotes the output voltage.

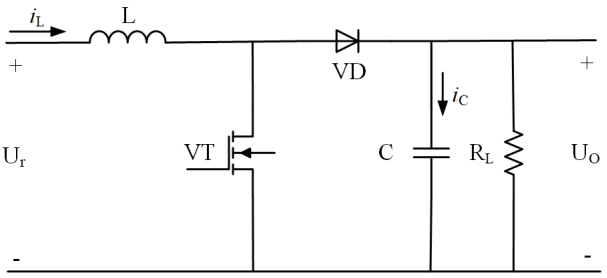

FIGURE 3. The model of the boost circuit.

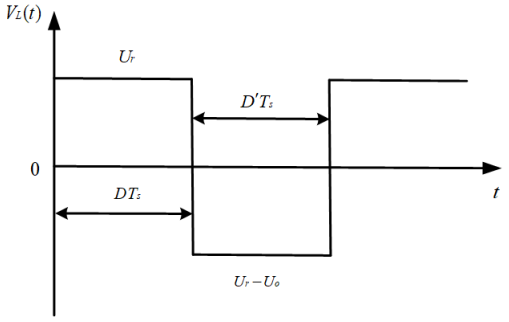

FIGURE 4. The relationship between inductance, voltage and time.

C. THE BOOST CIRCUIT

In this subsection, the boost circuit is an important part of UPS to provide stable DC voltage for the inverter, and the model of the boost circuit is shown in Fig. 3, in which, let L, VT, VD, C and R_L denote the inductance, the MOSFET, the freewheeling diode, and the filter capacitor, and the load resistance, respectively. U_r denotes the rectified voltage. i_L and i_C are the current through L_1 and C_2. Let U_o denote the output voltage of the boost circuit.

We assume that D and $D' = 1 - D$ denote the duty cycle, and T_s is cycling time. When VT is on, $0 \le t \le DTs(D < 1)$, as shown in (1). When VT is off, $DTs \le t \le Ts(D < 1)$, as shown in (2). Fig. 4 shows the relationship between the inductance, the voltage and the time. Fig. 5 shows the relationship between the capacitance, the current and the time.

$$\begin{cases} V_L = L\dfrac{di_L(t)}{dt} = U_r \\ i_C = C\dfrac{dU_o(t)}{dt} = -\dfrac{U_o(t)}{R_L} \end{cases} \tag{1}$$

$$\begin{cases} L\dfrac{di_L(t)}{dt} = U_r(t) - U_o(t) \\ C\dfrac{dU_o(t)}{dt} = i_L(t) - \dfrac{U_o(t)}{R_L} \end{cases} \tag{2}$$

From Fig. 4 and Fig. 5, from 0 to T_s, the relationship between V_L, i_C and T_s is shown in (3).

$$\begin{cases} \displaystyle\int_0^{T_S} V_L(t)d(t) = U_r DT_S + (U_r - U_o)D'T_S \\ \displaystyle\int_0^{T_S} i_C(t)d(t) = -\frac{U_o}{R_L}DT_S + \left(i_L - \frac{U_o}{R_L}\right)D'T_S \end{cases} \tag{3}$$

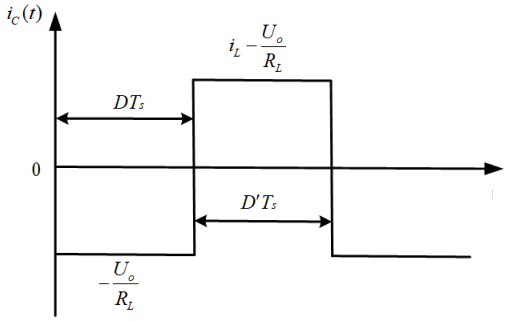

FIGURE 5. The relationship between capacitance, current and time.

In order to obtain the relationship between U_o, U_r, and i_L in (4) with the constrain that (3) is equal to zero.

$$\begin{cases} \dfrac{U_o}{U_r} = \dfrac{1}{D'} \\ i_L = \dfrac{U_r}{D'^2 R_L} \end{cases} \tag{4}$$

Assume that τ denotes the time constant. The segmented equation of V_L and i_C can be expressed by (5).

$$\begin{cases} V_L = \dfrac{1}{T_s}\left[\displaystyle\int_0^D V_L(\tau)d(\tau) + \int_0^{T_s} V_L(\tau)d(\tau)\right] \\ i_C = \dfrac{1}{T_s}\left[\displaystyle\int_0^D i_C(\tau)d(\tau) + \int_0^{T_s} i_C(\tau)d(\tau)\right] \end{cases} \tag{5}$$

V_L and i_C are substituted into (5), which can be obtained (6) by using the average variable instead of instantaneous variable.

$$\begin{cases} L\dfrac{di_L(t)}{dt} = U_r - D'U_o \\ C\dfrac{dU_o(t)}{dt} = D'i_L - \dfrac{U_o}{R_L} \end{cases} \tag{6}$$

Then, (6) can be linearized, and set $(\bar{U}_r(t), \bar{i}_C(t), \bar{U}_o(t))$ as the static working point of boost, which consists of the DC component (U_r, i_C, U_o) and the AC small signal component $(\tilde{U}_r(t), \tilde{i}_C(t), \tilde{U}_o(t))$, these mathematical descriptions are shown in (7).

$$\begin{cases} \bar{U}_r(t) = U_r + \tilde{U}_r(t) \\ \bar{i}_C(t) = i_C + \tilde{i}_C(t) \\ \bar{U}_o(t) = U_o + \tilde{U}_o(t) \end{cases} \tag{7}$$

Next, $d(t) = D + \tilde{d}(t)$ is one of the part in the AC component $\tilde{d}(t)$. Substituting (7) into (6), it obtains

$$\begin{cases} L\dfrac{d\tilde{i}_L(t)}{dt} = \tilde{U}_r(t) - D'\tilde{U}_o(t) + U_o\tilde{d}(t) + \tilde{U}_o(t)\tilde{d}(t) \\ C\dfrac{d\tilde{U}_o(t)}{dt} = D'\tilde{i}_C(t) - \dfrac{\tilde{U}_o(t)}{R_L} - i_C\tilde{d}(t) - \tilde{U}_o(t)\tilde{d}(t) \end{cases} \tag{8}$$

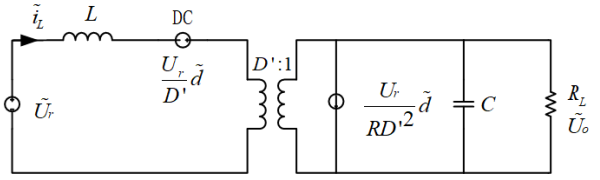

FIGURE 6. The small signal equivalent circuit of the boost circuit.

In addition, (8) can be linearized and removed the second order differential term, it obtains

$$\begin{cases} L\dfrac{d\tilde{i}_L(t)}{dt} = \tilde{U}_r(t) - D'\tilde{U}_o(t) + U_o\tilde{d}(t) \\ C\dfrac{d\tilde{U}_o(t)}{dt} = D'\tilde{i}_C(t) - \dfrac{\tilde{U}_o(t)}{R_L} - i_C\tilde{d}(t) \end{cases} \tag{9}$$

Then, the equivalent circuit of boost circuit is established by (9), and it is shown in Fig. 6.

In Fig. 6, the transfer function G_{oi} can be obtained the mathematical relationship between U_r and U_o. (11), (12) and (13) represent the transfer function between U_o and the duty cycle, the transfer function between i_L and the duty cycle, the transfer function between i_L and U_r, respectively.

$$G_{oi} = \frac{\tilde{U}_o(s)}{\tilde{U}_i(s)} = \frac{D'}{LCs^2 + \frac{L}{R_L}s + D'^2} \tag{10}$$

$$G_{od} = \frac{\tilde{U}_o(s)}{\hat{d}(s)} = \frac{U_r - \frac{U_r L}{D'^2 R_L}s}{LCs^2 + \frac{L}{R_L}s + D'^2} \tag{11}$$

$$G_{id}(s) = \frac{\tilde{i}_L(s)}{\tilde{d}(s)} = \frac{U_o Cs + \frac{2U_o}{R}}{LCs^2 + \frac{L}{R_L}s + D'^2} \tag{12}$$

$$G_{ir}(s) = \frac{\tilde{i}_L(s)}{\tilde{U}_r(s)} = \frac{Cs + \frac{1}{R}}{LCs^2 + \frac{L}{R_L}s + D'^2} \tag{13}$$

D. THE INVERTER CIRCUIT

This subsection mainly introduces the inverter circuit, and the physical model is shown in Fig. 7, in which, let U_o, U_n, C, U denote the output voltage of the boost circuit, the output voltage of the inverter circuit, the capacitor, the load voltage, respectively. Moreover, L_1 and L_2 are the full-bridge rectifier diodes, r_{s_1} and r_{s_2} are the equivalent resistance of the inductance. In addition, the output load can be divided into the fixed load and the distributed one. The fixed load can be regarded as an ideal resistive one, ignoring the inductance and the resistance r_s. Let i_C and U be the input ($x = [U, i_c]^T$ and $\dot{x} = \begin{bmatrix} \dot{U} \\ \dot{i}_C \end{bmatrix}$) and y be the output. The state equation can be established in (14).

$$\begin{cases} \dot{x} = \begin{bmatrix} 0 & \frac{1}{C} \\ -\frac{r_s}{LR} - \frac{1}{L} & -\frac{1}{RC} - \frac{r_s}{L} \end{bmatrix} x + \begin{bmatrix} 0 \\ \frac{1}{L} \end{bmatrix} u \\ y = \begin{bmatrix} 1 & 0 \end{bmatrix} x \end{cases} \tag{14}$$

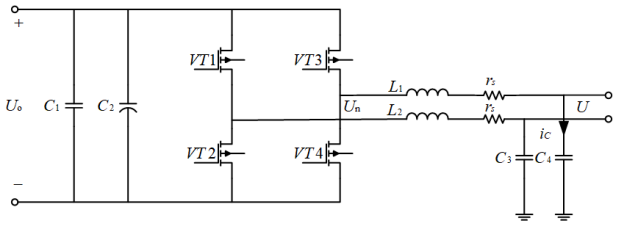

FIGURE 7. The model of the inverter circuit.

Then, the output voltage U in (15) can be obtained by (14).

$$U = \frac{1}{LCs^2 + \left(RC + \frac{L}{r_s}\right)s + \left(1 + \frac{r_s}{R}\right)} U_n \tag{15}$$

However, when the load has disturbance, the current i flowing through the load can be regarded as disturbance variable, the capacitor voltage U and capacitor current i_c are regarded as state variables, U_n is the input variables, and y is the output variables. The state space can be established from Fig. 7, and (17) can be obtained by (16) through S-transforming.

$$\begin{cases} \dot{x} = \begin{bmatrix} 0 & \frac{1}{C} \\ -\frac{1}{L} & -\frac{r}{L} \end{bmatrix} x + \begin{bmatrix} 0 \\ \frac{1}{L} \end{bmatrix} U_n + \begin{bmatrix} -\frac{1}{C} \\ 0 \end{bmatrix} i \\ y = \begin{bmatrix} 1 & 0 \end{bmatrix} x \end{cases} \tag{16}$$

$$U = \frac{1}{LCs^2 + RCs + 1} U_n + \frac{-Ls - r_s}{LCs^2 + r_sCs + 1} i_C \tag{17}$$

E. PROBLEM STATEMENT

The power factor of UPS is not high in boost circuit; in addition, the output response of the inverter is slow, and the waveform of the output AC is not smooth and delayed, resulting in a great impact on the output of the inverter by the load.

III. THE DESIGNED CIRCUIT AND PROPOSED ALGORITHM

A. THE ACTIVE POWER FACTOR CORRECTION CIRCUIT

In UPS system, many researchers do not consider the power loss in the DC-DC converter [30]–[35], and the relevant control strategies are complex [20]–[24]. The energy storage inductor is in the boost circuit, resulting in a phase difference between the input current and the input voltage, the decrease of the power factor, and the loss of conversion power. Therefore, the active power factor correction (APFC) circuit is proposed, adopting the double closed-loop control system with the inner-loop (current) and the outer-loop (voltage), to adjust the duty cycle of VT and to improve the system's efficiency. In addition, the designed APFC circuit is shown in Fig. 8. The inner-loop, the outer-loop, and the simulation model are shown in Fig. 9, 10 and 11, respectively.

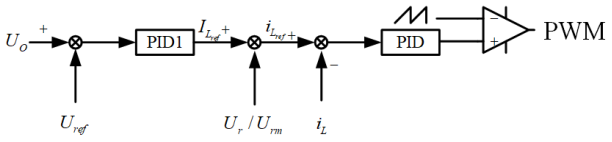

FIGURE 8. The designed active power factor correction circuit.

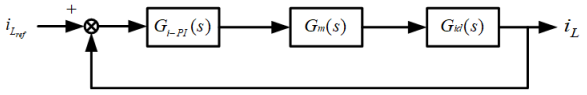

FIGURE 9. The model of the inner-loop (current).

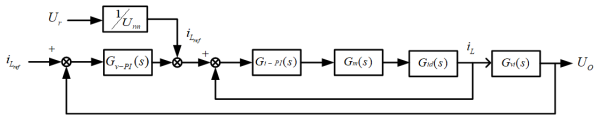

FIGURE 10. The model of the outer-loop (voltage).

The open-loop transfer function of the inner-loop (current) is in (18).

$$\begin{cases} \Phi_i(s) = G_{i-PI}(s) \cdot G_m(s) \cdot G_{id}(s) \\ G_{i-PI}(s) = k_{pi} + \dfrac{k_{ii}}{s} \\ G_m(s) = \dfrac{1}{U_m} \\ G_{id}(s) = \dfrac{U_oCs + \frac{2U_o}{R}}{LCs^2 + \frac{L}{R_L}s + D'^2} \end{cases} \tag{18}$$

where $G_{i-PI}(s)$ is the transfer function of current loop modulator, $G_m(s)$ is the transfer function of PWM modulator, $G_{id}(s)$ is the transfer function of inductance current to duty cycle, and U_m is the trigonometric amplitude value.

In Fig. 10, the open-loop transfer function of the voltage loop can be expressed in (19), in which, $G_{v-PI}(s)$ denotes the transfer function of the voltage regulator, $G_{vi}(s)$ denotes the transfer function of output voltage to inductance current.

$$\begin{cases} \Phi_v(s) = G_{v-PI}(s) \cdot \dfrac{\Phi_i(s)}{1 + \Phi_i(s)} \cdot G_{vi}(s)\dfrac{U_r}{U_{rm}} \\ G_{v-PI}(s) = k_{pv} + \dfrac{k_{iv}}{s} \\ G_{vi}(s) = \dfrac{G_{oi}(s)}{G_{ir}(s)} = \dfrac{U_r}{2CU_os} \end{cases} \tag{19}$$

B. THE FUZZY PID PARAMETER SELF-TUNING ALGORITHM

This subsection mainly introduces the fuzzy PID parameter self-turning algorithm. Some control strategies have been proposed, such as the synovial control, the robust continuous control, the model predictive control, and the neural network [30]–[36], but these control approaches are complex. Moreover, Ref. [42] proposed a new uni-polar boost inverter topology; in the designed inverter, it used the direct zero vector to realize the boost regulation of DC bus voltage and made the output AC voltage higher than the input DC voltage. There is one problem that the power factor of the DC chain

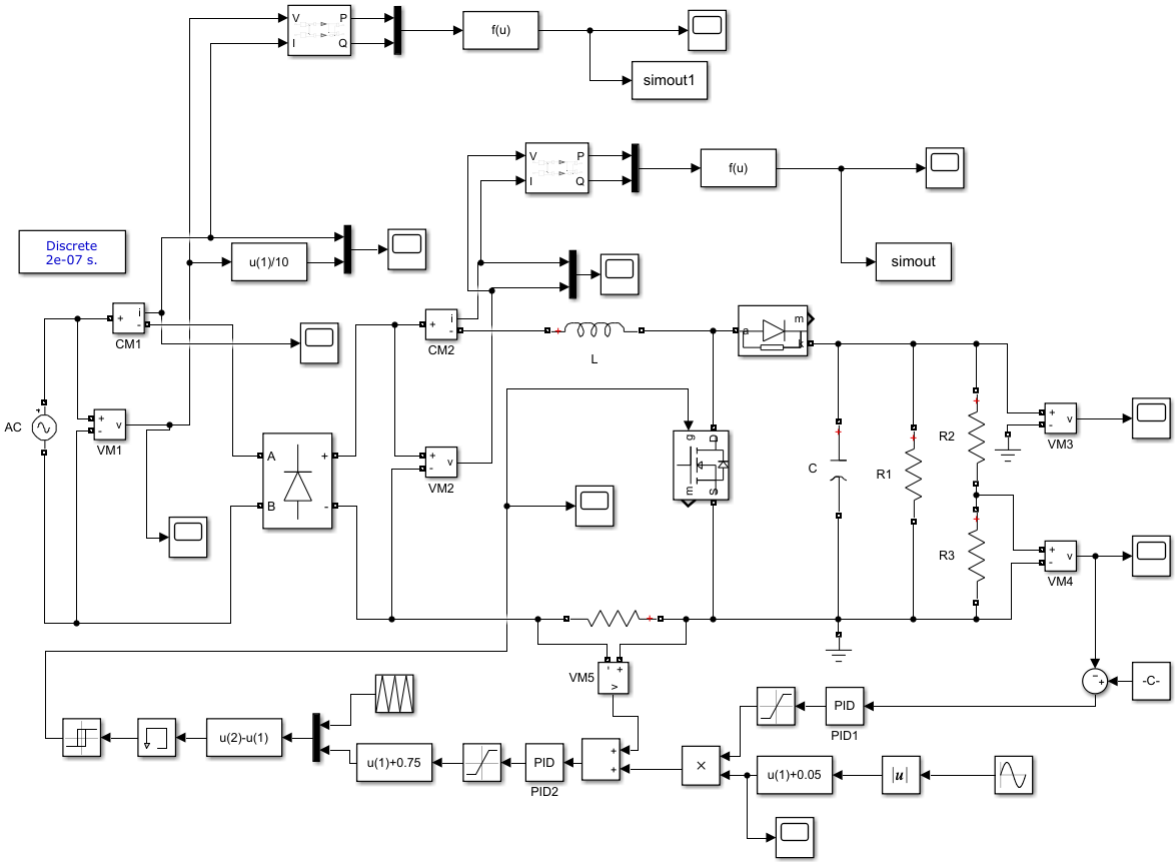

FIGURE 11. The simulation of APFC correction in the boost circuit.

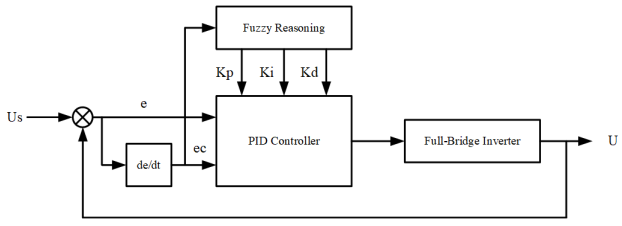

FIGURE 12. The model of the fuzzy PID controller.

TABLE 1. The fuzzy PID control rule with k_p.

e \ ec	NB	NM	NS	ZO	PS	PM	PB
NB	PB	PB	PM	PM	PS	ZO	ZO
NM	PB	PB	PM	PS	PS	ZO	NS
NS	PM	PM	PM	PS	ZO	NS	NS
ZO	PM	PM	PS	ZO	NS	NM	NM
PS	PS	PS	ZO	NS	NS	NM	NM
PM	PS	ZO	NS	NM	NM	NM	NB
PB	ZO	ZO	NM	NM	NM	NB	NB

and the utilization rate of the UPS system could be reduced because the uncontrollable rectifier supplies the DC power to the DC chain, and this power is supplied to the bridge of the inverter by coulping inductance. Therefore, the fuzzy PID algorithm is proposed to solve the following problem by adjusting the duty cycle of PWM in MOSFET to output the stable voltage.

The PID parameter self-tuning can continuously track the output voltage by comparing the fuzzy relationship among proportion k_p, integration k_i, differential k_d, error e and error change rate ec in the fuzzy PID control algorithm. The current PID can be modified in real time by fuzzy rule table reasoning. In addition, the model of the designed fuzzy PID controller is shown in Fig. 12, in which, the output voltage from AC power to the load can be controlled by the proposed algorithm to output the constant AC voltage in UPS system.

The fuzzy reasoning adaptive PID controller is designed, in which, U_s is the settling voltage of the inverter; U is the actual output voltage; the error e and the error change rate ec are the inputs; Δk_p, Δk_i, and Δk_d are the outputs. The tables of the control rule in the fuzzy PID controller are shown in Table 1, Table 2 and Table 3, in which, *NM*, *NS*, *ZO*, *PS*, *PM* and *PB* are seven fuzzy levels, which shows negative big, negative middle, negative small, zero, positive small, positive middle, and positive big, respectively.

When the PID controller obtains the current output voltage in the inverter, the voltage error e can be obtained by subtracting the reference voltage, then it can be discretized and divided into several different levels by the fuzzy PID rules.

Firstly, k_p mainly affects the response speed of the system. If k_p is larger, the response speed is faster, but, a larger

TABLE 2. The fuzzy PID control rule with k_i.

e \ ec	NB	NM	NS	ZO	PS	PM	PB
NB	NB	NB	NM	NM	NS	ZO	ZO
NM	NB	NB	NM	NS	NS	ZO	ZO
NS	NB	NM	NS	NS	ZO	PS	PS
ZO	NM	NM	NS	ZO	PS	PM	PM
PS	NM	NS	ZO	PS	PS	PM	PB
PM	ZO	ZO	PS	PS	PM	PB	PB
PB	ZO	ZO	PS	PM	PM	PB	PB

TABLE 3. The fuzzy PID control rule with k_d.

e \ ec	NB	NM	NS	ZO	PS	PM	PB
NB	PS	NS	NB	NB	NB	NM	PS
NM	PS	NS	NB	NM	NM	NS	ZO
NS	ZO	NS	NM	NM	NS	NS	ZO
ZO	ZO	NS	NS	NS	NS	NS	ZO
PS	ZO	ZO	ZO	ZO	ZO	ZO	ZO
PM	PB	NS	PS	PS	PS	PS	PB
PB	PB	PM	PM	PM	PS	PS	PB

k_p causes overshoot and oscillation of the system. If k_p is too small, the response speed will slow down, and the system's adjustment time will be prolonged, resulting in the deterioration of the static and dynamic characteristics of the system.

In addition, k_i mainly eliminates the steady-state error of the system. If k_i is too large, the static error will be eliminated quickly and the integral saturation phenomenon will occur at the initial of the response process, which can cause a larger response overshoot. If k_i is too small, the static error will be difficult to eliminate completely, which directly affects the adjustment accuracy of the system.

Then, k_d mainly improves the dynamic characteristics of the system, it can restrain the deviation from changing in any directions during the response process and it can also control the deviation in advance. If k_d is larger, the response process of the system will brake ahead of time, resulting in prolonging system's adjustment time and reducing system's anti-interference ability.

Moreover, if error e is smaller, the system will choose the larger k_p, k_i and k_d. At the same time, the anti-interference performance of the system needs to be considered to avoid the oscillation phenomenon. If e is larger, the fuzzy PID controller selects a larger k_p, a smaller k_i and k_d in the system's initial period to improve the system's response, to avoid excessive overshoot, and to prevent system's integral saturation.

Finally, if the error change rate ec is smaller, the system will choose a larger k_d. Otherwise, it a smaller k_d will be chosen.

Remark 1: The fuzzy PID controller is proposed in this paper. According to the dynamic tracking of the input signal, the designed fuzzy PID controller uses fuzzy control rules and self-reasoning algorithm to adjust the PID parameters in real-time, so that the system has a strong adaptability.

TABLE 4. The designed parameters in the boost circuit.

U_r	25.443/24 V
U_o	63 V
L	1.5 mH
C	7500 uF
R_1	50.7 Ω
R_2	511 $k\Omega$
R_3	10 $k\Omega$
Sampling Resistance of Current	35 $m\Omega$
Power Factor	0.996-1.0000

TABLE 5. The designed parameters in the inverter circuit.

U	36 V		
U_o	63 V DC	U_s	36 V AC
L_1	120 mH	L_2	120 mH
C_1	4.7 uF	C_2	4.7 uF
r_{s_1}	0.17 Ω	r_{s_2}	0.17 Ω

C. THE OUTPUT INTERFERENCE SOLUTION IN THE INVERTER

The output filter of the inverter can be considered as a low-pass filter, it needs to eliminates the unwanted high-frequency components. The power loss, transmitted by the bandwidth, should be as low as possible. Therefore, in this subsection, the LC low-pass filter is adopted on the output of the inverter instead of the RC filter.

There exists the noise, the high-frequency interference and the distortion on the inverter's output. In order to reduce interference, an isolation transformer is added to eliminate the loop interference of the system. The SPWM frequency of the inverter selects at 30 kHz to avoid using a high-frequency SPWM, it also introduces the high-frequency switching subharmonic interference, reduces the switching loss, and improves power utilization efficiency.

IV. EXPERIMENTAL RESULTS AND ANALYSIS

A. EXPERIMENT SET UP

The combination of simulation and actual experiment are implemented in this subsection to verify the effectiveness of the proposed APFC correction circuit and the fuzzy PID control algorithm. The low voltage single phase online UPS system consists of the rectifier circuit, the boost circuit, the inverter circuit, and the fuzzy PID controller. The rectifier circuit comprises a rectifier bridge module, in which, the input voltage is 18V AC and the output voltage is 25.443V DC. The boost circuit supplies 25.443V DC to 63V DC. The inverter circuit inverts 63V DC to 36V AC. The designed parameters of the boost circuit and the inverter circuit are shown in Table 4 and Table 5. In addition, the physical structure of the whole system is shown in Fig. 13.

B. THE BOOST CIRCUIT ANALYSIS

1) THE POWER FACTOR ANALYSIS

The simulation via MATLAB is shown in Fig. 14, in which, the blue line represents the power factor with APFC correction, and the red line shows the power factor without APFC correction. Fig. 14 shows that the power factor fluctuates

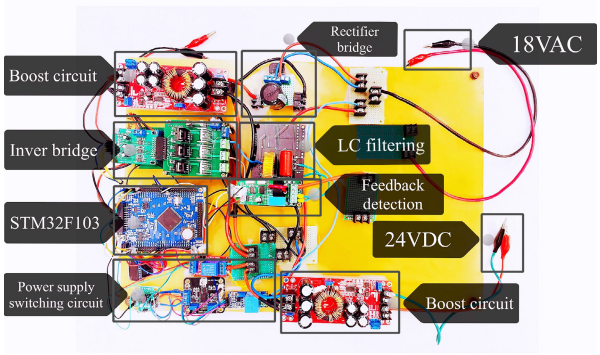

FIGURE 13. The physical model of the whole system.

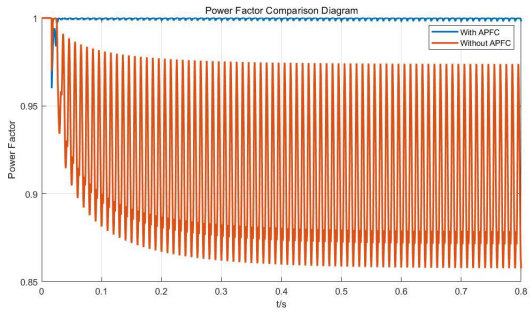

FIGURE 14. The power factor analysis.

between 0.857 and 0.973, which is extremely unstable, and the power factor is low. Because of the absence of APFC correction, the voltage and current phase difference are large in the boost circuit, making the power factor fluctuate in a certain range. Then, the power factor greatly improves and reaches more than 0.996. Therefore, the power factor, the utilization rate of power, and the power supply quality are improved, and the power supply of inverter is much more stable than before, and the high harmonic pollution of the power grid is also reduced.

2) THE VOLTAGE AND CURRENT ANALYSIS IN THE BOOST CIRCUIT

It can be seen from Fig. 15 that the analysis of voltage and current with APFC correction is conducted. The blue line represents the current waveform. In the first four cycles, the current changes greatly when the circuit is turned on. With the increase of the charging capacity of the energy storage element, the current decreases slowly, and it tends to be stable after the energy storage element is fully charged. Moreover, the red line shows the voltage waveform. In order to observe the waveform characteristics of the simulation experiment, the amplitude of the input voltage reduces to one-tenth of the origin. After adding APFC correction, the phase of voltage and that of current are the same, and their frequency is also the same so that the power factor is close to 1.

Then, Fig. 16 shows the analysis of voltage and current without APFC correction. The blue line shows the current waveform. When the APFC correction circuit is turned on, the current is substantial at the moment and it reaches more

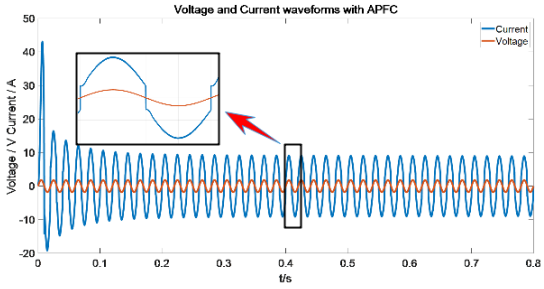

FIGURE 15. The voltage and current analysis with APFC correction.

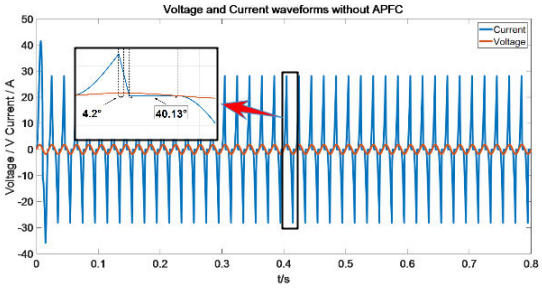

FIGURE 16. The voltage and current analysis without APFC correction.

than 40A. At the same time, the capacitor and inductor need to be charged and the current is tremendous. When the capacitor and inductor are fully charged, the current tends to be stable. Moreover, the red line shows the voltage waveform without APFC correction. In order to observe the waveform characteristics of the simulation experiment, the amplitude of the input voltage is reduced to one tenth of the original. It can be seen in Fig. 16 that the phase difference between the peak and peak of voltage and the peak and peak of current is 4.2°, but the phase difference between voltage zero crossing and current zero crossing is 40.13°, and the waveform of current is similar to triangular wave and the peak is very large.

Compared with Fig. 15 and Fig. 16, the waveform phases of voltage and current are the same, and the current waveform is smooth, and the peak value is much smaller than that without APFC correction. According to $P = UI$ (P is the power, U is the input voltage, and I is the input current), under the same condition, the boost circuit with APFC saves more power, greatly reduces the power loss of the circuit, and reduces the harmonic pollution to the power grid.

In the system, the input voltage is 18V AC (50Hz). After rectification, the output voltage is 25.443V DC. The fuzzy PID control algorithm is used to track the output voltage, which can be stabilized around 63V DC. Even if the power supply turns off, the DC voltage is also provided by the backup battery, and the output voltage can still be stable at 63V DC. As shown in Fig. 17, the blue line shows the output voltage with APFC correction, and the red line shows the output voltage without APFC correction. Moreover, at the initial time, these two curves are almost synchronous, the waveform of the voltage is smoother, and the output ripple is small.

Based on the above experimental analysis, it can be seen that the circuit without APFC correction will produce

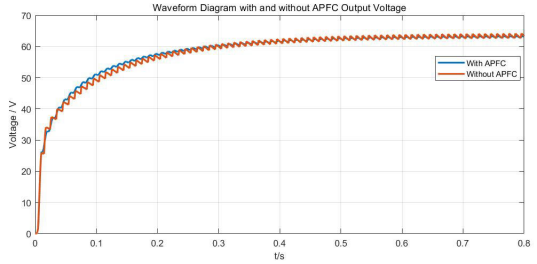

FIGURE 17. The output voltage waveform with and without APFC correction.

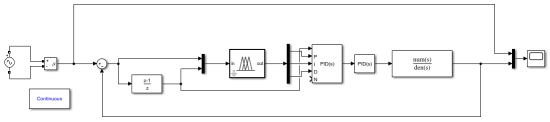

FIGURE 18. The model of the fuzzy PID controller in the inverter circuit.

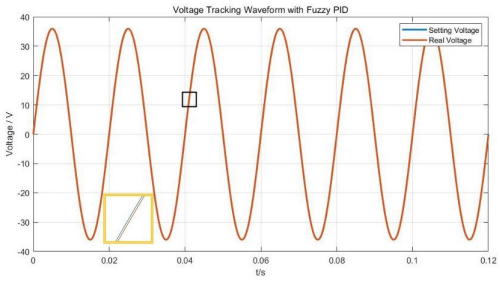

FIGURE 19. The voltage tracking curve under the fuzzy PID control algorithm.

high-frequency switching subharmonics due to the high-frequency on-off of the switch tube, which will pollute the power supply of the power grid, distort the voltage waveform of the public power grid, reduce the power quality, and threaten the safe and economic operation of various electrical equipment, including the power grid and capacitors. In addition, the low power factor affects the stability of the system, increases the loss of line power supply, and reduces the utilization of equipment. In the boost circuit, the APFC method of the voltage-current double closed loop is used to improve the power factor. The input current of the circuit is entirely continuous and can be modulated in the whole sinusoidal period of the input voltage so that a high power factor can be obtained; the current passing through the inductor is the input current. The peak current of the input current continuous switching transistor is small, and it has strong adaptability to the change of input voltage.

Remark 2: The boost circuit with APFC correction has better performance and higher power factor; in addition, APFC can save energy, reduce the harmonic pollution of the power grid, effectively reduce the power loss and improve power utilization efficiency.

C. THE INVERTER CIRCUIT ANALYSIS

The fuzzy PID control strategy is adopted to adjust the duty cycle of PWM in real-time, and then stabilize the output voltage at 36V AC. The inverter circuit is simulated through

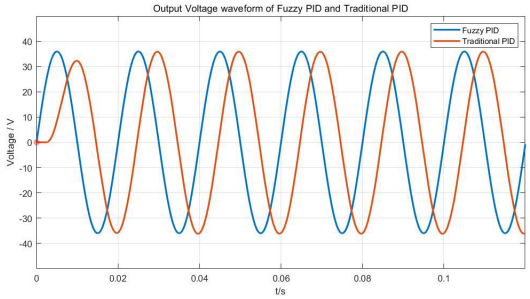

FIGURE 20. The output voltage waveform of the inverter under the fuzzy PID control algorithm.

MATLAB. As shown in Fig. 18, the input voltage is set to 63V DC. The output voltage can be stabilized at 36V AC, and the load is supplied by a PWM duty cycle controlled by the fuzzy PID control algorithm. The simulation result can be shown in Fig. 19 and the transfer function of the inverter is designed in (20).

$$G_f = \frac{314370499.3525}{s^2 + 35531914.647s + 314401939.5464} \tag{20}$$

In Fig. 19, the red line shows the output voltage with the fuzzy PID controller, and it almost completely tracks the reference voltage in the output frequency, the amplitude, and the phase. However, the output and input voltage have small differences and these can be even negligible. It shows that the output voltage can be adjusted quickly and accurately by applying the fuzzy PID control algorithm to adapt the amplitude of output voltage when the load suddenly changes.

It can be seen from Fig. 20, the blue line shows the output voltage under the fuzzy PID control strategy, and the yellow line shows the output voltage under the traditional PID controller. The output response under the fuzzy PID control algorithm is rapid with no delay, the amplitude reaches 36V, and the frequency can reach 50 Hz in one duty cycle. But, the output response by traditional PID is slower, and it needs at least two duty cycles to output 36V AC (50 Hz).

Remark 3: The fuzzy PID control strategy in the inverter can improve the response speed, enhance the anti-interference ability of inverter, and enhance the robustness of the system. When the load changes, it can optimize the power quality and make its frequency and amplitude more stable.

Remark 4: The proposed fuzzy PID control strategy has the advantages in strong portability and reliability, so it is not only suitable for the inverter with 63V DC input, but also suitable for other inverter with high-voltage DC input. In addition, the proposed control algorithm has strong robustness, it can resist the external interference, and can also improve the output response speed of the inverter and provide high-quality AC power for the loads.

D. THE LOAD CHANGE ANALYSIS ON THE UPS SYSTEM

This subsection mainly analyses the load change on the UPS system. From Table 6, the load adjustment rate is calculated in (21). When the load current changes from 0.1A to 1.2A, the

TABLE 6. The influence of load change on output voltage.

Load current (A)	Load voltage (V)	Input power (W)	Output power (W)	Efficiencyη (%)
0.1	35.99	4.1700	3.5990	86.30
0.2	35.99	8.3050	7.1980	86.67
0.3	36.00	12.3600	10.8000	87.38
0.4	36.00	17.1600	14.4000	83.92
0.6	36.00	25.8300	21.6000	83.62
0.8	35.99	34.4500	28.7920	83.58
0.9	36.01	38.4500	32.4090	84.29
1.0	36.01	42.2200	36.0100	85.29
1.2	36.01	50.2000	43.2120	86.07

TABLE 7. The influence of input voltage change on output voltage.

DC input voltage (V)	Load voltage (V)	Load current (A)	Input power (W)	Output power (W)	Efficiencyη (%)
14	36.00	0.40	17.4700	14.4000	82.42
16	36.00	0.40	18.2500	14.4000	78.90
18	36.01	0.40	17.7100	14.4040	81.33
20	36.01	0.40	17.2800	14.4040	83.36
22	35.99	0.40	17.4200	14.3960	82.64
24	36.01	0.40	16.9900	14.4040	84.78
26	35.99	0.40	16.8500	14.3960	85.44
28	36.00	0.40	17.1400	14.4000	84.01
30	36.02	0.40	16.5600	14.4080	87.00

TABLE 8. Comparison of power factor and THD in output voltage. (X means the data is not mentioned.)

Reference	Power Factor	THD	Reference	Power Factor	THD	Reference	Power Factor	THD
[13]	0.99	9.2%	[14]	0.96	X	[15]	X	X
[16]	0.98	3.74%	[17]	0.98	17.8%	[18]	0.91	21%
[19]	0.968	X	[20]	0.9	X	[21]	X	X
[22]	X	X	[23]	X	X	[24]	0.9	X
[25]	0.85	5%	[26]	X	1.25%	[27]	X	1.25%
[28]	X	X	[29]	X	0.05%	[30]	X	X
[31]	X	3%	[32]	X	X	[33]	X	X
[34]	X	0.87%	[35]	X	X	[36]	X	5%
[37]	0.97	X	[38]	X	0.3%	[39]	0.995	X
[40]	X	X	[41]	X	0.86%	[42]	X	0.8%
This Paper	0.996	0.54%						

voltage fluctuation is around 35.99V AC to 36.01V AC, and the efficiency remains between 83.56% and 87.38%, which indicates that the output voltage of the UPS system can be stable at 36V AC when the load changes.

$$S_I = \frac{|U_{o(0.1A)} - U_{o(1.2A)}|}{36} \times 100\% = 0.056\%. \quad (21)$$

E. THE INPUT VOLTAGE ANALYSIS ON THE UPS SYSTEM

This subsection mainly analyses the input voltage changed on the UPS system. According to Table 7, the voltage regulation rate can be calculated in (22). When the output voltage of the uncontrollable rectifier bridge fluctuates between 14V DC and 30V DC (the self-coupling transfer passes through the isolation transformer, simulates the grid voltage fluctuation, and then passes the rectifier), the output voltage of the load maintains between 35.99V AC and 36.01V AC, and the efficiency maintains from 78.90% to 87.00%. It shows that the system still makes the output stability of the AC power supply to the load when the input voltage fluctuates and the system has strong robustness.

$$S_U = \frac{|U_{o(30V)} - U_{o(14V)}|}{36} \times 100\% = 0.083\%. \quad (22)$$

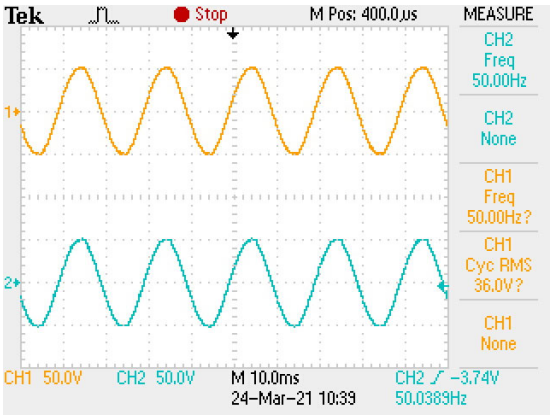

FIGURE 21. The waveform of load voltage and load current.

Fig. 21 shows the waveform of the load voltage and the load current, in which, the channel 1 (CH1) shows the output voltage of the load and the channel 2 (CH2) represents the output current of the load. It can be seen from Fig. 21 that the load voltage is 36V AC (50 Hz). When the load is resistive, the voltage and current are in phase.

F. COMPARISON OF POWER FACTOR AND THD IN OUTPUT VOLTAGE

In this subsection, the comparison of power factor and THD in output voltage is analyzed. Let V_{THD-F} define the THD of the output voltage in (23), in which, $V_{h,rms}$ denotes the effective value of second harmonic component and above of output voltage, and $V_{1,rms}$ denotes the effective value of the fundamental component.

$$V_{THD-F} = \sqrt{\frac{\sum_{h=2}^{N} {V_{h,rms}}^2}{{V_{1,rms}}^2}} \tag{23}$$

The active power factor correction proposed in this paper can improve the power factor of the boost part to 0.996, which is closer to 1 than that in the references list shown in Table 8, and the THD of output voltage reaches 0.54%. In addition, compared with the references in Table 8, the proposed control strategy can improve the working efficiency, eliminate the harmonic interference to the power grid when UPS works, reduce the total current and the power loss of the system. It can stabilize the load voltage, improve the quality of AC power output by UPS, and provide efficient and reliable AC power supply for the loads.

V. CONCLUSION

The voltage and current double closed-loop AFPC correction circuit and the fuzzy PID control algorithm are proposed in this paper. In the boost circuit of UPS system, the power factor can reach above 0.996 under APFC correction. This correction circuit can improve the utilization of electric energy, greatly reduce the line power loss, and improve the quality of the power supply. Using the fuzzy PID control algorithm in the inverter can enhance the robustness of the system, optimize the AC quality, make its frequency and amplitude more stable.

However, this paper only studies the control strategy of single-phase UPS, and lacks the research experiment of three-phase UPS; the power consumption of the load and the human-computer interaction are not monitored. In the future, the single UPS can be further studied to the three-phase. In human-computer interaction, the load power parameters can be detected in real time through the host computer. In addition, the output voltage of the UPS system will increase to 220V or 380V, and the battery charging circuit and control strategy can be studied and tested.

REFERENCES

[1] A. Karpati, G. Zsigmond, M. Voros, and M. Lendvay, "Uninterruptible power supplies (UPS) for data center," in *Proc. IEEE 10th Jubilee Int. Symp. Intell. Syst. Informat.*, Sep. 2012, pp. 351–355, doi: 10.1109/SISY.2012.6339543.

[2] L. M. A. Caseiro, A. M. S. Mendes, and S. M. A. Cruz, "Cooperative and dynamically weighted model predictive control of a 3-level uninterruptible power supply with improved performance and dynamic response," *IEEE Trans. Ind. Electron.*, vol. 67, no. 6, pp. 4934–4945, Jun. 2020, doi: 10.1109/TIE.2019.2921283.

[3] A. Pievatolo, E. Tironi, and I. Valade, "Semi-Markov Processes for power system reliability assessment with application to uninterruptible power supply," *IEEE Trans. Power Syst.*, vol. 19, no. 3, pp. 1326–1333, Aug. 2004, doi: 10.1109/TPWRS.2004.826756.

[4] D. P. Devanathan and S. Irrusapparajan, "A survey of harmonic distortion and reduction techniques," *Int. J. Pharmacy Technol.*, vol. 8, no. 4, pp. 23581–23589, Dec. 2016.

[5] H. Komurcugil, N. Altin, S. Ozdemir, and I. Sefa, "Lyapunov-function and proportional-resonant-based control strategy for single-phase grid-connected VSI with LCL filter," *IEEE Trans. Indus. Electron.*, vol. 63, no. 5, pp. 2838–2849, May 2016, doi: 10.1109/TIE.2015.2510984.

[6] M. Aamir and S. Mekhilef, "An online transformerless uninterruptible power supply (UPS) system with a smaller battery bank for low-power applications," *IEEE Trans. Power Electron.*, vol. 32, no. 1, pp. 233–247, Jan. 2017, doi: 10.1109/TPEL.2016.2537834.

[7] Q. Lin, F. Cai, W. Wang, S. Chen, Z. Zhang, and S. You, "A high-performance online uninterruptible power supply (UPS) system based on multitask decomposition," *IEEE Trans. Ind. Appl.*, vol. 55, no. 6, pp. 7575–7585, Nov. 2019, doi: 10.1109/TIA.2019.2935929.

[8] J. Lu, M. Savaghebi, S. Golestan, J. C. Vasquez, J. M. Guerrero, and A. Marzabal, "Multimode operation for on-line uninterruptible power supply system," *IEEE J. Emerg. Sel. Topics Power Electron.*, vol. 7, no. 2, pp. 1181–1196, Jun. 2019, doi: 10.1109/JESTPE.2018.2842436.

[9] V. de Souza, S. A. O. da Silva, and L. B. G. Campanhol, "A line-interactive UPS system operating with optimized power processing in backup mode," in *Proc. 21st Eur. Conf. Power Electron. Appl. (EPE ECCE Eur.)*, Sep. 2019, p. 10, doi: 10.23919/EPE.2019.8914813.

[10] S. S. H. Bukhari, T. A. Lipo, and B.-I. Kwon, "An online UPS system that eliminates the inrush current phenomenon while feeding multiple load transformers," *IEEE Trans. Ind. Appl.*, vol. 53, no. 2, pp. 1149–1156, Mar. 2017, doi: 10.1109/TIA.2016.2622229.

[11] A. Kumar and P. M. Kurulkar, "Power supply systems for defence applications a review—Part-I: Gensets," in *Proc. Nat. Power Electron. Conf. (NPEC)*, Dec. 2017, pp. 276–282, doi: 10.1109/NPEC.2017.8310471.

[12] E. Sunarno, I. Sudiharto, I. Ferdiansyah, S. D. Nugraha, O. A. Qudsi, and M. G. Muhammad, "Design of single phase full bridge inverter for uninterruptible power supply (UPS)," in *Proc. 2nd Int. Conf. Appl. Inf. Technol. Innov. (ICAITI)*, Sep. 2019, pp. 27–31, doi: 10.1109/ICAITI48442.2019.8982151.

[13] J. Y. Lee, K. W. Heo, K. T. Kim, and J. H. Jung, "Analysis and design of three-phase buck rectifier employing UPS to supply high reliable DC power," *Energies*, vol. 13, no. 7, pp. 1–12, 2020, doi: 10.3390/en13071704.

[14] H. Jing, Z. Weiying, and L. Jinhong, "Study on improving EMC of APFC converter with chaotic spread-spectrum technique," in *Proc. IEEE 2nd Adv. Inf. Technol., Electron. Autom. Control Conf. (IAEAC)*, Mar. 2017, pp. 433–437, doi: 10.1109/IAEAC.2017.8054051.

[15] S. Hong, H. Cheng, and P. Zeng, "N-K constrained composite generation and transmission expansion planning with interval load," *IEEE Access*, vol. 5, pp. 2779–2789, 2017.

[16] N. A. Rahman, K. Kamarudin, and R. Baharom, "Boost active power factor correction converter using various current controllers in double loop control algorithm," in *Proc. IEEE Int. Conf. Power Energy (PECon)*, Dec. 2020, pp. 24–28, doi: 10.1109/PECon48942.2020.9314613.

[17] C. Zhao, J. Zhang, and X. Wu, "An improved variable on-time control strategy for a CRM flyback PFC converter," *IEEE Trans. Power Electron.*, vol. 32, no. 2, pp. 915–919, Feb. 2017, doi: 10.1109/TPEL.2016.2594201.

[18] N. Vazquez, C. Aguilar, J. Arau, R. O. Caceres, I. Barbi, and J. A. Gallegos, "A novel uninterruptible power supply system with active power factor correction," *IEEE Trans. Power Electron.*, vol. 17, no. 3, pp. 405–412, May 2002, doi: 10.1109/TPEL.2002.1004248.

[19] A. Abramovitz, "Effect of the ripple current on power factor of CRM boost APFC," in *Proc. CES/IEEE 5th Int. Power Electron. Motion Control Conf.*, Aug. 2006, pp. 1–4, doi: 10.1109/IPEMC.2006.4778222.

[20] Q. Zhang, Y. Li, J. Yang, and J. Yang, "An active boost type APFC power management circuit," in *Proc. 29th Chin. Control Decis. Conf. (CCDC)*, May 2017, pp. 7034–7038, doi: 10.1109/CCDC.2017.7978450.

[21] Y. Hashemi, H. Abdolrezaei, and B. Hashemi, "Coordination of generation and reactive power expansion planning considering APFC units," in *Proc. Int. Power Syst. Conf. (PSC)*, Dec. 2019, pp. 490–496, doi: 10.1109/PSC49016.2019.9081517.

[22] J. Lu, J. M. Guerrero, M. Savaghebi, A. M. Y. M. Ghias, Y. Guan, X. Hou, and J. C. Vasquez, "An effective solution for regeneration protection in uninterruptible power supply," *IEEE Trans. Ind. Appl.*, vol. 55, no. 3, pp. 3055–3065, May 2019, doi: 10.1109/TIA.2019.2900601.

[23] D. Shahzad, S. Pervaiz, N. Zaffar, and K. K. Afridi, "Control of a GaN-based high-power-density single-phase online uninterruptible power supply," in *Proc. 20th Workshop Control Modeling Power Electron. (COMPEL)*, Jun. 2019, pp. 1–6, doi: 10.1109/COMPEL.2019.8769700.
[24] A. N. Kumle, S. H. Fathi, and M. Inanloo, "Z-source online UPS," in *Proc. 6th Power Electron., Drive Syst. Technol. Conf. (PEDSTC)*, Feb. 2015, pp. 621–626, doi: 10.1109/PEDSTC.2015.7093346.
[25] B. Tamyurek, "A high-performance SPWM controller for three-phase UPS systems operating under highly nonlinear loads," *IEEE Trans. Power Electron.*, vol. 28, no. 8, pp. 3689–3701, Aug. 2013, doi: 10.1109/TPEL.2012.2227817.
[26] I. Muhammad, A. Muhammad, W. Asad, B. M. Fahad, and A. Imtiaz, "Line-interactive transformerless uninterruptible power supply (UPS) with a fuel cell as the primary source," *Energies*, vol. 11, no. 3, pp. 1–19, Mar. 2018, doi: 10.3390/en11030542.
[27] A. Muhammad, U. T. Wajahat, A. K. Kafeel, A. M. Mudasir, and M. Saad, "A high-frequency isolated online uninterruptible power supply (UPS) system with small battery bank for low power applications," *Energies*, vol. 150, no. 4, pp. 1–20, Mar. 2017, doi: 10.3390/en10040418.
[28] M. Tinkir, U. Onen, M. Kalyoncu, and F. M. Botsali, "Pid and interval type-2 fuzzy logic control of double inverted pendulum system," in *Proc. 2nd Int. Conf. Comput. Autom. Eng. (ICCAE)*, Feb. 2010, pp. 117–121, doi: 10.1109/ICCAE.2010.5451988.
[29] Z. W. Liu, J. P. Luo, and G. R. Zhu, "Design and implementation of online uninterruptible power supply system based on STM32," in *Proc. 6th Int. Conf. Adv. Energy Resour. Environ. Eng.*, vol. 647. Chongqing, China, 2021, pp. 1–5, doi: 10.1088/1755-1315/647/1/012009.
[30] S. Károly and K. Péter, "Mathematical basis of sliding mode control of an uninterruptible power supply," *Acta Polytechnica Hungarica*, vol. 11, no. 3, pp. 87–106, 2014.
[31] D. Yahya, "Model predictive control of uninterruptible power supply with robust disturbance observer," *Energies*, vol. 12, no. 15, pp. 1–22, Jul. 2019, doi: 10.3390/en12152871.
[32] Q. J. Dong, "Discussion on control strategy of UPS inverter," *Telecom Power Technol.*, vol. 35, no. 10, pp. 29–33, 2018, doi: 10.19399/j.cnki.tpt.2018.10.012.
[33] L. X. Ma, L. Y. Ji, and Y. J. Zhu, "Embedded power control system based on neural network PID," *Control Eng. China*, no. 1, pp. 597–584, 2019, doi: 10.14107/j.cnki.kzgc.20190716.
[34] I. Sudiharto, F. D. Murdianto, E. Sunarno, S. D. Nugraha, and O. A. Qudsi, "Design and implementation unipolar SPWM full-bridge inverter using fuzzy Sugeno in DC microgrid isolated system," in *Proc. 3rd Int. Conf. Inf. Technol., Inf. Syst. Electr. Eng. (ICITISEE)*, Nov. 2018, pp. 368–373, doi: 10.1109/ICITISEE.2018.8721032.
[35] Z. R. Zhang, "Design of numericial control UPS power supply based on 51 single-chip," *Telecom Power Technol.*, vol. 35, no. 1, pp. 16–18, 2018, doi: 10.19399/j.cnki.tpt.2018.01.007.
[36] M. Mohamadian, A. Abrishamifar, M. Shahrdad, M. Arefian, and M. Fazeli, "Implementation of the first commercial medium power active front end transformerless uninterruptible power supply made in Iran," in *Proc. 7th Power Electron. Drive Syst. Technol. Conf. (PEDSTC)*, Feb. 2016, pp. 217–221, doi: 10.1109/PEDSTC.2016.7556864.
[37] V. Burlaka, S. Gulakov, S. Podnebennaya, and E. Kudinova, "Low-cost online uninterruptible power supply with input power factor correction and wide input voltage range," in *Proc. IEEE 7th Int. Conf. Energy Smart Syst. (ESS)*, May 2020, pp. 234–237, doi: 10.1109/ESS50319.2020.9160034.
[38] Y. Zhu, W. Hu, Z. Wang, and X. Ma, "Single-phase on-line uninterruptible power supply with low load regulation," in *Proc. IEEE Int. Conf. Power Electron., Comput. Appl. (ICPECA)*, Jan. 2021, pp. 615–619, doi: 10.1109/ICPECA51329.2021.9362585.
[39] Y.-S. Lai and Z.-J. Su, "Novel on-line maximum duty point tracking technique to improve two-stage server power efficiency and investigation into its impact on hold-up time," *IEEE Trans. Ind. Electron.*, vol. 61, no. 5, pp. 2252–2263, May 2014, doi: 10.1109/TIE.2013.2273479.
[40] S. A. O. da Silva, R. A. Modesto, A. F. Neto, and S. G. de Souza Cervantes, "A single-phase UPS system with harmonic suppression and reactive power compensation," in *Proc. Brazilian Power Electron. Conf.*, Sep. 2009, pp. 558–563, doi: 10.1109/COBEP.2009.5347745.
[41] R. Razi, M. Monfared, and A. Hadizadeh, "Tracking error minimization in multi-loop control of UPS inverters using the reference frame transformation," in *Proc. 8th Power Electron., Drive Syst. Technol. Conf. (PEDSTC)*, 2017, pp. 311–316, doi: 10.1109/PEDSTC.2017.7910343.
[42] Q. Yang, W. X. Huang, Y. W. Hu, Y. F. Zhou, and F. F. Bu, "A novel single stage boost inverter," *J. Trans. China Electrotech. Soc.*, vol. 26, no. 4, pp. 122–127, 2011, doi: 10.19595/j.cnki.1000-6753.tces.2011.04.019.

SHENGXIAN XU received the B.E. degree from the School of Information Science and Engineering, Dalian Polytechnic University, China, in 2020, where he is currently pursuing the M.E. degree. His current research interest includes the smart gird theory and applications.

CHEN LI (Member, IEEE) received the M. Eng.Sc. degree from the University of New South Wales (UNSW Sydney), Australia, in 2019. He is currently a Teaching Assistant with the School of Electrical Engineering and Telecommunications, UNSW Sydney. His current research interests include the theory and application of guidance, navigation, and control. He was an Invite Reviewer for several top journals, such as *IET Signal Processing*, IEEE Asian Journal of Control, *Journal of Information Technology and Control* (ITC), and *International Journal of Advanced Robotic Systems* (IJARS).

YURU WANG received the master's degree in engineering from the Dalian University of Technology, Dalian, China, in 1997. She is currently a Lecturer with the School of Information Science and Engineering, Dalian Polytechnic University, Dalian. Her research interests include the embedded applications and intelligent control research.

BAOYING LI (Member, IEEE) was born in 1965. He received the B.E. and M.E. degrees from the Dalian Institute of Light Industry (now Dalian Polytechnic University), in 1988 and 1994, respectively. He is currently an Associate Professor with Dalian Polytechnic University. His research interests include intelligent control and its application in unmanned systems.